Journal of Computational and Applied Mechanics, Vol. 19, No. 2, (2024), pp. 85–104
DOI: 10.32973/jcam.2024.004

THERMOELASTIC ANALYSIS OF FUNCTIONALLY GRADED ANISOTROPIC ROTATING DISKS AND RADIALLY GRADED SPHERICAL PRESSURE VESSELS

Dávid Gönczi
Institute of Applied Mechanics, University of Miskolc
Miskolc-Egyetemváros, H-3515 Miskolc, Hungary
mechgoda@uni-miskolc.hu

[Received: June 10, 2024; Accepted: August 23, 2024]

Abstract. This work deals with the thermoelastic problem of a functionally graded cylindrically anisotropic rotating disk with arbitrary thickness profile subjected to combined axisymmetric thermal and mechanical loads. The material properties are arbitrary functions of the radial coordinate and temperature. A coupled system of ordinary differential equations is derived and the boundary value problem is transformed to an initial value problem, the unknown functions are the stress function and the components of the displacement field. This method uses a state vector formalism to present an effective way to calculate the stress field within monoclinic, orthotropic or isotropic radially graded disks in plane stress state. An analytical solution is presented for the case when the orthotropic material parameters and the thickness profile are specific power-law functions of the radial coordinate and the temperature field is arbitrary. The developed numerical method is applied to simpler steady-state thermoelastic problems of functionally graded spherical pressure vessels, where the material properties are arbitrary functions of the temperature field and of the radial coordinate. The developed methods are compared and results obtained from finite element simulations.

Mathematical Subject Classification: 74S99, 74E05
Keywords: Anisotropic disk, thermomechanical analysis, thermal stresses

1. Introduction

Functionally graded materials (FGM) are advanced materials in which the composition gradually changes, resulting in a corresponding change in the material properties according to the function of the structural component, usually in one direction. The gradient interface between the constituent materials produces a smooth transition from one material to the next, which provides great favourable mechanical behaviour and thermal protection. Due to its excellent material properties, the concept of FGM has become more popular in recent years.

Many studies deal with the mechanics of functionally graded materials from various aspects. Numerous books give solutions to linearly elastic problems for non-homogeneous bodies such as [1–3]. Several papers presented analytical, semi-analytical and numerical solutions for thermomechanical problems of hollow spheres, cylinders,

beams and disks. Noda et. al. [4, 5] studied one-dimensional steady-state thermal stress problems for isotropic functionally graded hollow circular cylinders and spheres using the perturbation method, multilayered approach and Green functions. Chen and Lin [6] carried out an elastic analysis for thick cylinders and spherical pressure vessels made of functionally graded materials when the material parameters vary exponentially along the radial coordinate. Nayak et al. [7] and Bayat et al. [8] developed analytical solutions to obtain the radial, tangential and effective stresses within thick spherical pressure vessels made of FGMs subjected to axisymmetric mechanical and thermal loading. The material properties of the vessel depended on the radial coordinate as a power-law function but the Poisson's ratio had constant value. In a paper by Pen and Li [9] a steady-state thermoelastic problem of isotropic radially graded disks with arbitrary radial non-homogeneity was considered. The numerical solution was reduced to a solution of a Fredholm integral equation. A work by Stampouloglou and Theotokoglou [10] gave the exact solutions for a radially non-homogeneous hollow circular cylinder and disk with exponential and power-law based shear modulus and constant Poisson's ratio. The method used the nonhomogeneous compatibility equations of strain and the equilibrium equations of the thermoelastic problem in order to determine the reduced displacement and stresses in a functionally graded component. Jabbary et al. [11] and [12] dealt with the thermoelastic analysis of a functionally graded rotating thick shell with variable thickness subjected to thermo-mechanical loading by using higher-order shear deformation theory. The mechanical properties, except for the Poisson's ratio, are assumed to vary arbitrarily along the investigated spatial coordinate.

Paper [13] presented the displacement and stress fields in a radially graded hollow circular disk subjected to constant angular acceleration, Poisson's ratio and thermal loading. Here a semi-analytical approach was utilized. Boğa and Yildirim [14] solved these problems with the method of complementary functions and investigated parabolic thickness profiles. For isotropic functionally graded hollow circular disks with arbitrary material properties along the radial direction, Gönczi and Ecsedi [15] presented a numerical method to solve the steady-state thermoelastic problem. Similarly to these papers, there are a number of works dealing with isotropic, radially graded structural components, such as [16–19]. Studies [20, 21] by Zheng et al. determined the displacement and stress fields in a radially graded isotropic and fibre-reinforced rotating disks. The governing equations for displacement and normal stresses are solved using the finite difference method. A work by Eraslan et al. [22] presented analytical solutions of an orthotropic disk with a power-law function based profile. The basic equations are transformed into a standard hypergeometric differential equation by means of a suitable transformation, then an analytical solution is obtained in terms of hypergeometric functions.

A work by Tarn [23] derived exact solutions for the temperature field and thermoelastic stresses for inhomogeneous hollow and solid cylinders when some of the material parameters followed a power law distribution; furthermore, the cylinder was subjected to axial force. Sladek et. al. [24] presented a meshless method based on the local Petrov–Galerkin approach which was developed for the stress analysis of

two-dimensional, anisotropic, linearly elastic and viscoelastic solids with continuously varying material properties. The analysed domain was divided into small circular subdomains. In paper [25] the nonlinear steady-state heat conduction equation is solved using an iterative power-series method to obtain the temperature field, then the three-dimensional thermoelasticity equations are solved by a power-series solution procedure to determine the displacements and stresses in anisotropic radially graded hollow cylinders. A method is presented where the cylinder is divided into multiple sub-cylinders and the Taylor series is utilized. Chen et. al. [26] dealt with the axisymmetric problems of transversely isotropic elastic materials based on displacement functions, which were the functions of the thickness coordinate.

In Chang et al. [27] the basic equations of thermoelasticity were formulated into a state equation and a state space formalism for generalized anisotropic thermoelasticity accounting for thermomechanical coupling and thermal relaxation was developed. To obtain the solution for weak thermomechanical coupling the method of perturbation with multiple scales was used and the propagation of plane harmonic thermoelastic waves in an anisotropic medium was studied.

Ceniga [28] dealt with an analytical model of thermal stresses originating during the cooling process of an anisotropic solid continuum with uniaxial or triaxial anisotropy. The investigated continuum consisted of anisotropic spherical particles periodically distributed in an anisotropic infinite matrix. Beom [29] presented a formalism for the general solutions of in-plane thermoelastic fields that satisfy the equilibrium equation. An orthotropy rescaling technique is developed to determine the dependence of thermoelastic fields on the dimensionless orthotropy parameter. The complete thermoelastic fields for the original problem can be evaluated from the solutions of the transformed problem by linear transformation with orthotropy rescaling. Yildirim [30] presents a complementary function method to deal with the thermomechanical problem of orthotropic disks. Allam et. al. [31] presents semi-analytical methods to tackle special material distributions. Papers [32, 33] used discretized domains and a variational approach to tackle the problems of orthotropic disks. Besides disks and spherical bodies, functionally graded beams are often used in various engineering applications; papers such as [34, 35] tackle the mechanical analysis and buckling of such beams.

This paper deals with the steady-state thermoelastic problem of a radially graded anisotropic rotating disk and radially graded pressure vessels subjected to axisymmetric thermal and mechanical loads. As we have seen in the presented literature, the models of the axisymmetric disk and sphere problems contain some kinds of restrictions when it comes to — for example – the functions of the material properties, the thickness of the disk, or neglecting the temperature dependency. Our aim is to formulate a more general approach where all of the material properties are arbitrary functions of the radial coordinate r and temperature T, and a further aim is to present an effective way to calculate the stress field. The considered cylindrically anisotropic disk can be seen in Figure 1, where the material of the disk is a radially graded monoclinic material, while Figure 2 shows a sketch of the isotropic hollow spherical body.

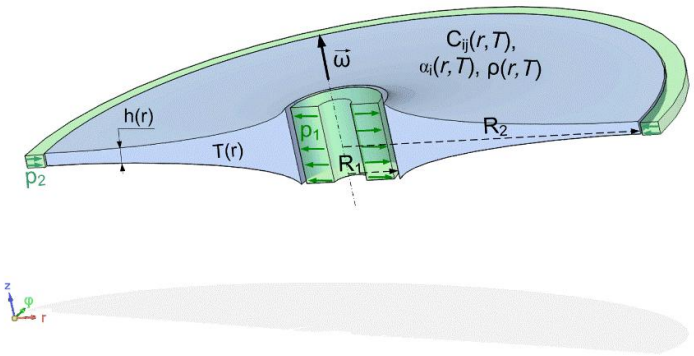

Figure 1. Sketch of a segment of the considered disk with the mechanical and thermal loads

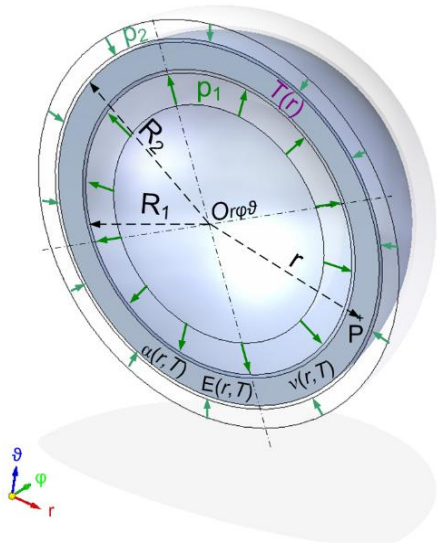

Figure 2. Sketch of a segment of the considered sphere with the mechanical and thermal loads

The thickness of the disk is denoted by $h(r)$, and it is an arbitrary function of the radial coordinate r, where $R_1 \leqslant r \leqslant R_2$, ω is the constant angular velocity. The thermal loading is an arbitrary temperature field $T(r)$ obtained from the solution of the steady-state heat conduction equation. The uniformly distributed mechanical loading exerted on the inner boundary surface is denoted by p_1, while p_2 is the pressure acting on the outer curved boundary surface. For these problems the thermoelastic equations of plane-stress state will be used. A new numerical approach is presented

which is based on a coupled system of first-order ordinary differential equations, where the unknown functions are the radial displacement and the stress function.

Anisotropy refers to the directional dependence of material properties. Due to the symmetry, the stiffness tensor $\mathfrak{C}$ contains 21 independent elastic constants.

$$\boldsymbol{\sigma} = \mathbf{C}\boldsymbol{\varepsilon} + \boldsymbol{\beta}T \tag{1a}$$

$$\begin{bmatrix} \sigma_1 \\ \sigma_2 \\ \sigma_3 \\ \tau_{13} \\ \tau_{23} \\ \tau_{12} \end{bmatrix} = \begin{bmatrix} \bar{C}_{11} & \bar{C}_{12} & \bar{C}_{13} & \bar{C}_{14} & \bar{C}_{15} & \bar{C}_{16} \\ & \bar{C}_{22} & \bar{C}_{23} & \bar{C}_{24} & \bar{C}_{25} & \bar{C}_{26} \\ & & \bar{C}_{33} & \bar{C}_{34} & \bar{C}_{35} & \bar{C}_{36} \\ & & & \bar{C}_{44} & \bar{C}_{45} & \bar{C}_{46} \\ & sym. & & & \bar{C}_{55} & \bar{C}_{56} \\ & & & & & \bar{C}_{66} \end{bmatrix} \begin{bmatrix} \varepsilon_1 \\ \varepsilon_2 \\ \varepsilon_3 \\ \gamma_{23} \\ \gamma_{13} \\ \gamma_{12} \end{bmatrix} + \begin{bmatrix} \bar{\beta}_1 \\ \bar{\beta}_2 \\ \bar{\beta}_3 \\ \bar{\beta}_4 \\ \bar{\beta}_5 \\ \bar{\beta}_6 \end{bmatrix} T \tag{1b}$$

where $\boldsymbol{\beta} = -\mathbf{S} \cdot \boldsymbol{\alpha}$, $\mathbf{S}$ is the material compliance tensor, α_i $(i = 1...6)$ are the coefficients of linear thermal expansion, and $\boldsymbol{\sigma}$ and $\boldsymbol{\varepsilon}$ denote the stress strain vectors, respectively. The different types of material anisotropy are determined by the existence of symmetries in the internal structure of the material. This reduces the number of independent stiffness coefficients (monoclinic materials have 13, orthotropic materials have 9, transversely isotropic materials have 5 and isotropic materials have 2 independent parameters) and thermal parameters β_i. In the investigated problems monoclinic materials will be considered. This means that there is one material symmetry plane and for example $C_{i4} = C_{4i} = 0$, $C_{i5} = C_{5i} = 0$, $C_{j6} = C_{6j} = 0$, $(i = 1, 2, 3$ and $j = 4, 5)$

2. Numerical method for disks

We consider a rotating radially graded cylindrically anisotropic disk as shown in Figure 1, and a cylindrical coordinate system $Or\varphi z$ will be used. The strain-displacement relations for disks are [1]:

$$\varepsilon_r(r) = \frac{du(r)}{dr}, \quad \varepsilon_\varphi(r) = \frac{u(r)}{r}, \quad \gamma_{r\varphi}(r) = \frac{dv(r)}{dr} - \frac{v(r)}{r}, \tag{2}$$

where $u = u(r)$ is the radial displacement, $v(r)$ is the tangential displacement, $\gamma_{r\varphi}(r)$ denotes the shear strain and $\varepsilon_r(r)$, $\varepsilon_\varphi(r)$ are the normal strains in the radial and circumferential directions, respectively. In the case of a plane-stress state the stress-strain relationships can be expressed with the following reduced material constants of monoclinic materials:

$$\begin{aligned}
&C_{11} = \bar{C}_{11} - \tfrac{\bar{C}_{13}}{\bar{C}_{33}}\bar{C}_{13};\ C_{12} = \bar{C}_{12} - \tfrac{\bar{C}_{23}}{\bar{C}_{33}}\bar{C}_{13};\ C_{16} = \bar{C}_{16} - \tfrac{\bar{C}_{36}}{\bar{C}_{33}}\bar{C}_{13};\ \beta_1 = \bar{\beta}_1 - \tfrac{\bar{\beta}_3}{\bar{C}_{33}}\bar{C}_{13};\\
&C_{21} = \bar{C}_{21} - \tfrac{\bar{C}_{31}}{\bar{C}_{33}}\bar{C}_{23};\ C_{22} = \bar{C}_{22} - \tfrac{\bar{C}_{23}}{\bar{C}_{33}}\bar{C}_{23};\ C_{26} = \bar{C}_{26} - \tfrac{\bar{C}_{36}}{\bar{C}_{33}}\bar{C}_{23};\ \beta_2 = \bar{\beta}_2 - \tfrac{\bar{\beta}_3}{\bar{C}_{33}}\bar{C}_{23};\\
&C_{61} = \bar{C}_{61} - \tfrac{\bar{C}_{31}}{\bar{C}_{33}}\bar{C}_{63};\ C_{62} = \bar{C}_{62} - \tfrac{\bar{C}_{32}}{\bar{C}_{33}}\bar{C}_{63};\ C_{66} = \bar{C}_{66} - \tfrac{\bar{C}_{36}}{\bar{C}_{33}}\bar{C}_{63};\ \beta_6 = \bar{\beta}_6 - \tfrac{\bar{\beta}_3}{\bar{C}_{33}}\bar{C}_{63}.
\end{aligned} \tag{3}$$

as

$$\sigma_r(r) = C_{11}(T,r)\varepsilon_r(r) + C_{12}(T,r)\varepsilon_\varphi(r) + C_{16}(T,r)\gamma_{r\varphi}(r) + \beta_1(T,r)T(r), \tag{4}$$

$$\sigma_\varphi(r) = C_{21}(T,r)\varepsilon_r(r) + C_{22}(T,r)\varepsilon_\varphi(r) + C_{26}(T,r)\gamma_{r\varphi}(r) + \beta_2(T,r)T(r), \tag{5}$$

$$\tau_{r\varphi}(r) = C_{61}(T,r)\varepsilon_r(r) + C_{62}(T,r)\varepsilon_\varphi(r) + C_{66}(T,r)\gamma_{r\varphi}(r) + \beta_6(T,r)T(r) \tag{6}$$

where σ_r and σ_φ $\tau_{r\varphi}$ are normal stresses, $\tau_{r\varphi}$ is shearing stress, $T(r) = T_a(r) - T_0$ is the temperature difference function, $T_a(r)$ is the absolute temperature, T_0 is the reference temperature, and C_{ij} $(i,j = 1,2,6)$ are stiffness coefficients. The time-independence of the functions involved separates the analysis of the temperature field from that of the elastic field, which means that the problem becomes uncoupled. Therefore the temperature field can be calculated separately from the heat conduction equations, and becomes an input function for this part of the model, which means that $C_{ij}(T(r),r) = C_{ij}(r) = C_{ji}(r)$ and $\beta_i(T(r),r) = \beta_i(r)$. Furthermore, the shearing stress $\tau_{r\varphi}$ is zero due to the axisymmetry, boundary conditions and

$$\frac{\mathrm{d}}{\mathrm{d}r}(rh\tau_{r\varphi}) + h\,\tau_{r\varphi} = 0, \qquad \rightarrow \quad h\tau_{r\varphi} = \frac{F}{r^2}, \rightarrow \quad F = \tau_{r\varphi} = 0. \tag{7}$$

The equilibrium equation in the radial direction has the following form:

$$\frac{\mathrm{d}}{\mathrm{d}r}\left[r\sigma_r(r)h(r)\right] - h(r)\sigma_\varphi(r) + h(r)\rho\omega^2 r^2 = 0\,, \tag{8}$$

where $h(r)$ is the thickness of the disk and ρ denotes the density, which depends on the radial coordinate and the temperature field. The general solution in terms of the stress function $V = V(r)$ is

$$\sigma_r(r) = \frac{1}{r}\frac{V(r)}{h(r)}, \tag{9}$$

$$\sigma_\varphi(r) = \frac{\mathrm{d}V(r)}{\mathrm{d}r}\frac{1}{h(r)} + \rho(r)\omega^2 r^2. \tag{10}$$

After lengthy manipulations of equations (4)-(10) the following system of ordinary differential equations can be derived for the displacement field and the stress function in cylindrically anisotropic radially graded disks:

$$\frac{\mathrm{d}}{\mathrm{d}r}\begin{bmatrix} u \\ V \\ v \end{bmatrix} = \begin{bmatrix} L^f_{11} & L^f_{12} & 0 \\ L^f_{21} & L^f_{22} & 0 \\ L^f_{31} & L^f_{32} & L^f_{33} \end{bmatrix}\begin{bmatrix} u \\ V \\ v \end{bmatrix} + \begin{bmatrix} L^T_{11} \\ L^T_{12} \\ L^T_{13} \end{bmatrix} T + \begin{bmatrix} 0 \\ -\omega^2 h\rho r^2 \\ 0 \end{bmatrix}, \tag{11}$$

$$\frac{\mathrm{d}}{\mathrm{d}r}\mathbf{f} = \mathbf{L}^f\mathbf{f} + \mathbf{L}^T T + \mathbf{L}^\omega, \tag{12}$$

where the following notations were introduced:

$$
\begin{gathered}
L_{01}=\frac{C_{12}C_{66}-C_{16}C_{62}}{C_{11}C_{66}-C_{16}^2},\ L_{11}^f(r)=-L_{01}\frac{1}{r},\ L_{12}^f(r)=\frac{C_{66}}{C_{11}C_{66}-C_{16}^2}\frac{1}{hr},\\
L_{21}^f(r)=\left[C_{22}-C_{21}L_{01}+C_{26}\left(\frac{C_{16}}{C_{66}}L_{01}-\frac{C_{26}}{C_{66}}\right)\right]\frac{h}{r},\ L_{22}^f(r)=L_{01}\frac{1}{r},\\
L_{31}^f(r)=\left(\frac{C_{16}}{C_{66}}L_{01}-\frac{C_{26}}{C_{66}}\right)\frac{1}{r},\ L_{32}^f(r)=\left(\frac{-C_{16}}{C_{11}C_{66}-C_{16}^2}\right)\frac{1}{hr},\ L_{33}^f(r)=\frac{1}{r},\\
L_{11}^T(r)=-\frac{C_{66}\beta_1-C_{16}\beta_6}{C_{11}C_{66}-C_{16}^2},\ L_{13}^T(r)=\frac{-C_{16}L_{11}^T}{C_{66}}-\frac{\beta_6}{C_{66}},\\
L_{12}^T(r)=\left(\beta_2+C_{21}L_{11}^T+C_{26}L_{13}^T\right)h,\\
C_{ij}(r,T(r)),\ \beta_i(r,T(r)),\ \rho(r,T(r));\quad i=1,2,6.
\end{gathered}
\tag{13}
$$

For isotropic radially graded disks the following expressions are used:

$$
\begin{gathered}
L_{11}^f(r)=\frac{-\nu(r,T)}{r},\ L_{12}^f(r)=\frac{1-[\nu(r,T)]^2}{E(r,T)hr},\\
L_{21}^f(r)=E(r,T)\frac{h}{r},\ L_{22}^f(r)=-L_{11}^f(r),\\
L_{31}^f(r)=L_{32}^f(r)=L_{33}^f(r)=L_{13}^T(r)=v(r)=0,\\
L_{11}^T(r)=\alpha(r,T)\left[1+\nu(r,T)\right],\ L_{12}^T(r)=-E(r,T)\alpha(r,T)h,
\end{gathered}
\tag{14}
$$

where $E(r,T(r))=E(r)$ is the Young's modulus, $\alpha(r,T(r))=\alpha(r)$ is the coefficient of linear thermal expansion and $v(r,T(r))=v(r)$ denotes the Poisson ratio. The next phase is the determination of the initial values for the system of differential equations (11). The stress boundary conditions of the rotating disk can be expressed in terms of the stress function as

$$
\sigma_r(R_1)=-p_1,\quad \sigma_r(R_2)=-p_2,
\tag{15}
$$

$$
V(R_1)=-p_1R_1h_1,\quad V(R_2)=-p_2R_2h_2,
\tag{16}
$$

where h_1 and h_2 are the thickness values at the inner and outer cylindrical boundary surfacesQ. Our aim is to formulate an initial value problem for the coupled system of differential equations (11). Two numerical solutions $[u_I(r);V_I(r)]$ and $[u_{II}(r),V_{II}(r)]$ are needed to determine the initial values of the considered two-point boundary value problem. The system of equations is reduced to:

$$
\frac{\mathrm{d}}{\mathrm{d}r}u=L_{11}^fu+L_{12}^fV+L_{11}^TT,\quad \frac{\mathrm{d}}{\mathrm{d}r}V=L_{21}^fu+L_{22}^fV+L_{21}^TT-\omega^2h\rho r^2.
\tag{17}
$$

For the calculations, the fourth-fifth order Runge-Kutta-Fehlberg method will be used in our numerical examples. The input values for the system of differential equations (17) are shown in Table 1. The initial values for the displacements are different arbitrary values, for the stress functions the stress boundary condition — equation (16) – is used.

Table 1. Numerical solution of the thermoelastic problems

Calculations of the initial values		Input values for $u(r)$		Input values for $V(r)$
Calc. I	Eqns. (17)	$u_I(R_1) = u_1$	u_1 (arbitrary)	$V_I(R_1) = -p_1 R_1 h_1$
Calc. II	Eqns. (17)	$u_{II}(R_1) = u_2$	$u_2 \neq u_1$	$V_{II}(R_1) = -p_1 R_1 h_1$
Final Problem	Eqns. (11)	u_3	Calculated with equation (18)	$V_I(R_1) = -p_1 R_1 h_1$

Using the solutions of calculations I and II, the initial value for the displacement field of the original problem can be computed as

$$u(R_1) = u_3 = u_1 + \frac{(u_2 - u_1)\left[-p_2 R_2 h_2 - V_I(R_2)\right]}{V_{II}(R_2) - V_I(R_2)}. \tag{18}$$

The validity of this statement follows from the linearity of the considered thermoelastic boundary value problem. With the displacement field and the stress function, the normal stresses and displacement field can be determined with equation (9) and

$$\sigma_\varphi(r) = \left(L_{21}^f u + L_{22}^f V + L_{21}^T T\right) h^{-1}. \tag{19}$$

3. Numerical method for spherical pressure vessels

A one-dimensional steady-state thermoelastic problem of an isotropic functionally graded spherical hollow body is considered. The spherical pressure vessel is subjected to arbitrary radial coordinate dependent thermal loading $T(r)$ and constant pressures p_1 and p_2 at the curved boundary surfaces, as we can see in Figure 2. The material properties are arbitrary functions of the radial coordinate and temperature. For this spherically symmetric problem a spherical coordinate system $Or\varphi\vartheta$is used. The strain-displacement and stress-strain relations can be expressed as [1]

$$\varepsilon_r(r) = \frac{du(r)}{dr}, \quad \varepsilon_\varphi(r) = \varepsilon_\vartheta(r) = \frac{u(r)}{r}, \tag{20}$$

$$\sigma_r(r) = \frac{E(r,T)}{[1+\nu(r,T)]\,[1-2\nu(r,T)]}\big\{[1-\nu(r,T)]\,\varepsilon_r r) + 2\nu(r,T)\varepsilon_\varphi(r) - \\ - \alpha(r,T)\,[1+\nu(r,T)]\,T(r)\big\}, \tag{21}$$

$$\sigma_\varphi(r) = \sigma_\vartheta(r) = \frac{E(r,T)}{[1+\nu(r,T)]\,[1-2\nu(r,T)]}\big\{\nu(r,T)\varepsilon_r(r) + \varepsilon_\varphi(r) - \\ - \alpha(r,T)\,[1+\nu(r,T)]\,T(r)\big\}. \tag{22}$$

The equilibrium equation in the radial direction can be written as

$$\frac{\mathrm{d}\sigma_r}{\mathrm{d}r} + \frac{2(\sigma_r - \sigma_\varphi)}{r} = 0, \tag{23}$$

therefore the general solution of equation (23) in terms of stress function $V(r)$ assumes the forms of

$$\sigma_r = \frac{V}{r^2}, \qquad \sigma_\varphi = \frac{1}{2r}\frac{\mathrm{d}V}{\mathrm{d}r}. \tag{24}$$

The system of ordinary differential equations can be expressed as

$$\frac{\mathrm{d}}{\mathrm{d}r}\begin{bmatrix} u \\ V \end{bmatrix} = \begin{bmatrix} -\frac{2\nu}{(1-\nu)}\frac{1}{r} & \frac{(1-2\nu)(1+\nu)}{(1-\nu)E}\frac{1}{r^2} \\ \frac{2E}{1-\nu} & \frac{2\nu}{1-\nu}\frac{1}{r} \end{bmatrix}\begin{bmatrix} u \\ V \end{bmatrix} + \begin{bmatrix} \frac{1+\nu}{1-\nu} \\ \frac{2E}{1-\nu}r \end{bmatrix}\alpha T. \tag{25}$$

We need three initial value calculations to solve this problem, similarly to our previously presented method. The steps of the solution and the input values can be seen in Table 2.

$$u_3 = u_1 + \frac{u_2 - u_1}{V_{II}(R_2) - V_I(R_2)}(-p_2 R_2^2 - V_I(R_2)). \tag{26}$$

Table 2. Numerical solution of the thermoelastic problems

Calculations of the initial values		Input values for $u(r)$		Input values for $V(r)$
Calc. I	Eq. (25)	$u_I(R_1) = u_1$	u_1 (arbitrary)	$V_I(R_1) = -p_1 R_1^2 = V_1$
Calc. II	Eqns. (25)	$u_{II}(R_1) = u_2$	$u_2 \neq u_1$	$V_{II}(R_1) = -V_1$
Final Problem	Eqns. (25)	u_3	Calculated with equation (26)	$V(R_1) = V_1$

After the third calculation, the radial normal stress can be calculated according to (24) and the tangential normal stress takes the form of

$$\sigma_\varphi = (1-\nu)^{-1}\left[E\frac{u}{r} + \nu\frac{V}{r^2} + E\alpha T\right]. \tag{27}$$

4. Analytical solution for orthotropic disks

An analytical solution will be derived for the case when the material properties of the cylindrically orthotropic, radially graded rotating disk follow the following power-law based distribution:

$$\begin{gathered} \rho(r) = \rho_0^0\left(\frac{r}{R_1}\right)^m = \rho_0 r^m, \quad \beta_i(r) = \beta_{i0}^0\left(\frac{r}{R_1}\right)^m = \beta_{i0} r^m, \\ C_{ij}(r) = C_{ij0}^0\left(\frac{r}{R_1}\right)^m = C_{ij0} r^m; \end{gathered} \qquad i,j = 1,2,6. \tag{28}$$

The thickness profile of the disk is described as $h(r) = h_0 r^w$, the temperature-dependency of the material properties is neglected in this case, but thermal loading comes from an arbitrary temperature field $T(r)$. The combination of the basic equations of thermoelasticity results in the following differential equations for the radial displacement field $u(r)$:

$$K_1\frac{\mathrm{d}^2 u}{\mathrm{d}r^2} + K_2\frac{\mathrm{d}u}{\mathrm{d}r} + K_3\frac{u}{r^2} + K_4\frac{T}{r} + \beta_{10}\frac{\mathrm{d}T}{\mathrm{d}r} + K_5 r = 0, \tag{29}$$

where we have introduced the constants

$$K_1 = C_{110}, \quad K_2 = C_{110}(m+w+1), \quad K_3 = C_{120}(m+w) - C_{220}, \\ K_4 = \beta_{10}(m+w+1) - \beta_{20}, \quad K_5 = \rho_0\omega^2. \tag{30}$$

The solution of (29) is

$$u(r) = C_1 r^{g_1} + C_2 r^{g_2} - \frac{r^{g_1}}{g_3}\int I_{T1}(r)\,\mathrm{d}r + \frac{r^{g_2}}{g_3}\int I_{T2}(r)\,\mathrm{d}r, \tag{31}$$

where C_1 and C_2 are integration constants, moreover

$$I_{T1}(r) = K_4 r^{-g_1} T(r) + K_5 r^{g_4} + \beta_{10} r^{g_5}\frac{\mathrm{d}T(r)}{\mathrm{d}r}, \\ I_{T2}(r) = K_4 r^{-g_2} T(r) + K_5 r^{g_5} + \beta_{10} r^{g_7}\frac{\mathrm{d}T(r)}{\mathrm{d}r}, \tag{32}$$

$$g_{1,2} = \frac{K_1 - K_2 \pm g_3}{2K_1}, \quad g_3 = \sqrt{(K_2-K_1)^2 - 4K_3K_1}\,, \\ g_{6,4} = \frac{3K_1 + K_2 \pm g_3}{2K_1}, \quad g_{7,5} = \frac{K_1 + K_2 \pm g_3}{2K_1}. \tag{33}$$

Substituting these results into equations (2), (4)-(6) we obtain the functions of the radial normal stress σ_r and tangential normal – or hoop – stress σ_φ:

$$\sigma_r(r) = C_1 S_{r;1}(r) + C_2 S_{r;2}(r) + S_{r;3}(r) + S_{r;4}(r), \tag{34}$$

$$\sigma_\varphi(r) = C_1 S_{\varphi;1}(r) + C_2 S_{\varphi;2}(r) + S_{\varphi;3}(r) + S_{\varphi;4}(r). \tag{35}$$

The following notations are used in equations (34) and (35):

$$S_{r;1}(r) = r^{m+g_1-1}(g_1 C_{110} + C_{120}), \\ S_{r;2}(r) = r^{m+g_2-1}(g_2 C_{110} + C_{120}), \\ S_{r;3}(r) = r^m\Bigg[(g_2 C_{110} + C_{120})\frac{r^{g_2-1}}{g_3}\int I_{T2}(r)\,\mathrm{d}r - \\ - (g_1 C_{110} + C_{120})\frac{r^{g_1-1}}{g_3}\int I_{T1}(r)\,\mathrm{d}r\Bigg], \\ S_{r;4}(r) = r^m\left[C_{110}\left(\frac{r^{g_2}}{g_3}I_{T2}(r) - \frac{r^{g_1}}{g_3}I_{T1}(r)\right) + \beta_{10}T(r)\right], \tag{36}$$

and

$$S_{\varphi;1}(r) = r^{m+g_1-1}(g_1 C_{120} + C_{220}), \\ S_{\varphi;2}(r) = r^{m+g_2-1}(g_2 C_{120} + C_{220}), \\ S_{\varphi;3}(r) = r^m\Bigg[(g_2 C_{120} + C_{220})\frac{r^{g_2-1}}{g_3}\int I_{T2}(r)\,\mathrm{d}r - \\ - (g_1 C_{120} + C_{220})\frac{r^{g_1-1}}{g_3}\int I_{T1}(r)\,\mathrm{d}r\Bigg], \\ S_{\varphi;4}(r) = r^m\left[C_{120}\left(\frac{r^{g_2}}{g_3}I_{T2}(r) - \frac{r^{g_1}}{g_3}I_{T1}(r)\right) + \beta_{20}T(r)\right]. \tag{37}$$

The constants of integrations can be calculated from the stress boundary conditions (15) as

$$C_1 = \frac{S_{r;2}(R_1)\,[p_2 + S_{r;3}(R_2) + S_{r;4}(R_2)] - S_{r;2}(R_2)\,[p_1 + S_{r;3}(R_1) + S_{r;4}(R_1)]}{S_{r;2}(R_2)S_{r;1}(R_1) - S_{r;2}(R_1)S_{r;1}(R_2)}, \quad (38)$$

$$C_2 = \frac{S_{r;1}(R_2)\,[p_1 + S_{r;3}(R_1) + S_{r;4}(R_1)] - S_{r;1}(R_1)\,[p_2 + S_{r;3}(R_2) + S_{r;4}(R_2)]}{S_{r;2}(R_2)S_{r;1}(R_1) - S_{r;2}(R_1)S_{r;1}(R_2)}. \quad (39)$$

In this case the circumferential displacement is zero $v(r) = 0$

Temperature field. For the determination of the temperature field we will consider the case when there are no internal heat sources, the constant temperature values of the cylindrical boundary surfaces t_1 and t_2 are given, moreover there are symmetric, radial coordinate dependent thermal boundary conditions of the third kind on the lower and upper boundary surfaces. This convective heat exchange is given by the temperature of the surrounding medium $t_{env}(r)$ and the heat exchange coefficient $\vartheta(r)$. According to Fourier's law of heat conduction, the heat flow can be expressed as

$$q_r = -\lambda_{11}\frac{\partial T}{\partial r} - \lambda_{12}\frac{1}{r}\frac{\partial T}{\partial \varphi}, \qquad q_\varphi = -\lambda_{12}\frac{\partial T}{\partial r} - \lambda_{22}\frac{1}{r}\frac{\partial T}{\partial \varphi}, \quad (40)$$

where λ_{11}, λ_{12} and λ_{22} are the coefficients of thermal conductance of the anisotropic material. In this axisymmetric case the temperature field $T(r)$ is the function of the radial coordinate. A multilayered approach will be used to determine the temperature field of the radially graded anisotropic disk with radial coordinate-dependent thermal conductivity. The concentric layers or subdomains have constant but different thicknesses and thermal conductivities $\lambda_{11} = \lambda$, the number of the layers is n, for the i-th layer the heat conduction equation takes the forms of [36]:

$$\nabla\,(t\mathbf{q}) + hT(r) = 0, \qquad \frac{\mathrm{d}^2 T_i}{\mathrm{d}r^2} + \frac{1}{r}\frac{\mathrm{d}T_i}{\mathrm{d}r} - {p_i}^2(T_i(r) - t_{env,\,i}) = 0, \quad (41)$$

where we have introduced the notation p_i as

$$R_{mi} = \frac{R_i + R_{i+1}}{2}, \quad \lambda_i = \lambda(R_{mi}), \quad h_i = h(R_{mi}), \quad \vartheta_i = \vartheta(R_{mi}), \ \text{ etc.} \quad (42)$$

The temperature values t_1 and $t_n + 1$ are given at the inner and outer radii of the disk, and the solution of the differential equation is

$$T_i(r) = \frac{(t_i - t_{envi})K_0(p_iR_{i+1}) - (t_{i+1} - t_{envi})K_0(p_iR_i)}{K_0(p_iR_{i+1})I_0(p_iR_i) - K_0(p_iR_i)I_0(p_iR_{i+1})}I_0(p_ir) + \\ + \frac{(-t_i - t_{envi})I_0(p_iR_{i+1}) + (t_{i+1} - t_{envi})I_0(p_iR_i)}{K_0(p_iR_{i+1})I_0(p_iR_i) - K_0(p_iR_i)I_0(p_iR_{i+1})}K_0(p_ir) + t_{env}(r), \quad (43)$$

where $I_0(x)$ and $K_0(x)$ are the modified Bessel functions of the first and second kind and of order zero. The surface temperatures of the adjacent layers are equal, the heat flow of the i-th layer q_i is constant, therefore we get the following equations for the disk:

$$t_{i+1} = T_i(R_{i+1}) = T_{i+1}(R_{i+1}), \quad h_i q_i(R_{i+1}) = h_{i+1} q_{i+1}(R_{i+1}) \quad i = 1, ..., n-1, \tag{44}$$

$$\begin{aligned} q_i(r) = &-\lambda_i p_i \frac{(t_i - t_{envi})K_0(p_i R_{i+1}) - (t_{i+1} - t_{envi})K_0(p_i R_i)}{K_0(p_i R_{i+1})I_0(p_i R_i) - K_0(p_i R_i)I_0(p_i R_{i+1})} I_1(p_i r) - \\ &- \lambda_i p_i \frac{(-t_i - t_{envi})I_0(p_i R_{i+1}) + (t_{i+1} - t_{envi})I_0(p_i R_i)}{K_0(p_i R_{i+1})I_0(p_i R_i) - K_0(p_i R_i)I_0(p_i R_{i+1})} K_1(p_i r) \\ &\qquad\qquad\qquad\qquad\qquad\qquad\qquad\qquad\qquad\qquad i = 1, ..., n-1 \end{aligned} \tag{45}$$

The unknown t_i temperature values can be calculated from (45). When there is no heat exchange on the upper and lower boundary surfaces and the temperature dependency is negligible, then the temperature distribution is:

$$T(r) = t_1 + \frac{t_2 - t_1}{\int\limits_{R_1}^{R_2} \frac{1}{\rho\lambda(\rho)} \mathrm{d}\rho} \int\limits_{R_1}^{r} \frac{1}{\rho\lambda(\rho)} \mathrm{d}\rho. \tag{46}$$

Similarly, when there are no internal heat sources and the temperature dependency of $\lambda(r)$ is negligible, the temperature field within spherical bodies can be expressed as:

$$T(r) = t_1 + \frac{t_2 - t_1}{\int\limits_{R_1}^{R_2} \frac{1}{\rho^2\lambda(\rho)} \mathrm{d}\rho} \int\limits_{R_1}^{r} \frac{1}{\rho^2\lambda(\rho)} \mathrm{d}\rho. \tag{47}$$

5. Numerical examples

There are multiple ways to calculate the effective material properties in temperature-dependent FGMs. For the numerical examples the following parameters will be used to describe the temperature dependency [37, 38]:

$$Ep(T) = P_0(P_{-1}T^{-1} + 1 + P_1 T + P_2 T^2 + P_3 T^3), \tag{48}$$

where E_p denotes a material property, P_i $(i = -1...3)$ are material dependent coefficients of temperature (usually T [K]), furthermore for radially graded two-component

disks and spheres the following expressions of effective material properties will be utilized:

$$Ep_f(r,T) = [Ep_1(T) - Ep_2(T)]\,[Z(r)]^m + Ep_2(T),$$
$$Z(r) = \frac{r - R_1}{R_2 - R_1}, \quad \text{or} \quad Z(r) = \frac{r}{R_1}, \tag{49}$$

where m is the volume fraction of the FGM and indices 1 and 2 denote the constituent materials in classic FGMs, steel, and ceramic materials.

Example 1. For the first numerical example, a thick radially graded steel–silicon nitride spherical pressure vessel with the following parameters is considered:

Table 3. Material parameters for the metal-ceramic FGM

Material property (E_p)	Metal (stainless steel)			
	P_{m0}	$P_{m1}(10^{-3})$	$P_{m2}(10^{-7})$	$P_{m3}(10^{-10})$
λ(W/mK)	15.39	−1.264	20.92	−7.223
α(1/k)	$12.33 \cdot 10^6$	0.8086	0.0	0.0
E(Pa)	$2.01 \cdot 10^{10}$	0.3079	−6.534	0.0
$V(-)$	0.3262	−0.1	3.797	0.0
Material property (E_p)	Ceramic (silicon nitride)			
	P_{c0}	$P_{c1}(10^{-3})$	$P_{c2}(10^{-7})$	$P_{c3}(10^{-10})$
λ(W/mK)	12.723	−1.032	5.466	−7.876
α(1/k)	$3.873 \cdot 10^6$	0.9095	0.0	0.0
E(Pa)	$3.484 \cdot 10^{10}$	−0.307	2.16	−8.946
$V(-)$	0.24	0.0	0.0	0.0

$$R_1 = 0.5 \text{ m}, \;\; R_2 = 0.59 \text{ m}, \;\; t_{inner} = 250 \text{ K}$$
$$t_{outer} = 20 \text{ K}, \;\; p_1 = 200 \text{ MPa}, \;\; p_2 = 10 \text{ MPa}, \;\; m = \{0.2,\, 1,\, 4\}$$

Three cases are investigated with three different volume fractions m. The temperature field in this case can be approximated as[39]:

$$T(r, m = 0.2) = 1.479 \cdot 10^5 r^2 - 3.27 \cdot 10^5 r + 2.701 \cdot 10^5 - 99427 r^{-1} + 13879.7 r^{-2}\ [K]\,,$$
$$T(r, m = 1) = 94650.7 r^2 - 2.15321 r + 183778 - 70336.8 r^{-1} + 10285.8 r^{-2}\ [K]\,,$$
$$T(r, m = 4) = 58516 r^2 - 1.1778 \cdot 10^5 r + 88658 - 30213.3 r^{-1} + 4069.9 r^{-2}\ [K]\,.$$

The calculations were checked by results obtained by finite element simulations with Abaqus. The 3D model was built from 32 homogeneous layers, and coupled temperature-displacement elements were used. They were in good agreement, although the FE solution oscillated significantly at the inner and outer radii of the sphere, which led to greater error. Figure 3 shows the radial displacements and Figure 4 contains the diagrams of the radial normal stresses (lower half between −200 and 10 MPa) and the tangential normal stresses, illustrated with thicker lines.

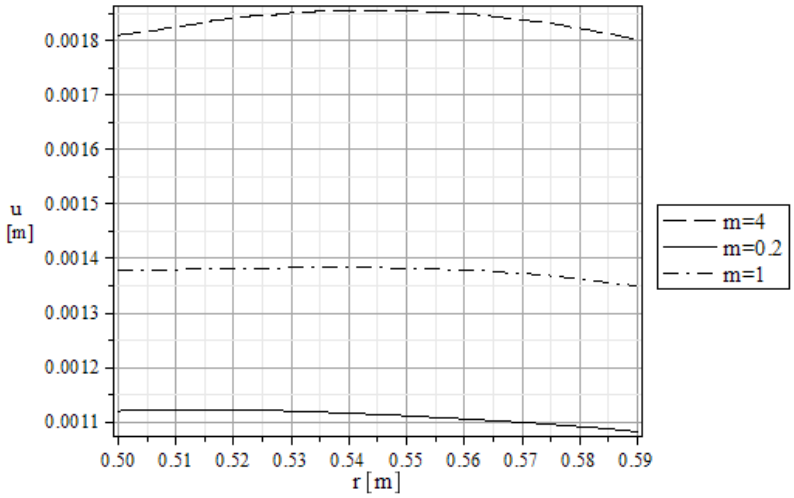

Figure 3. The radial displacements $u(r)$ of the spherical bodies

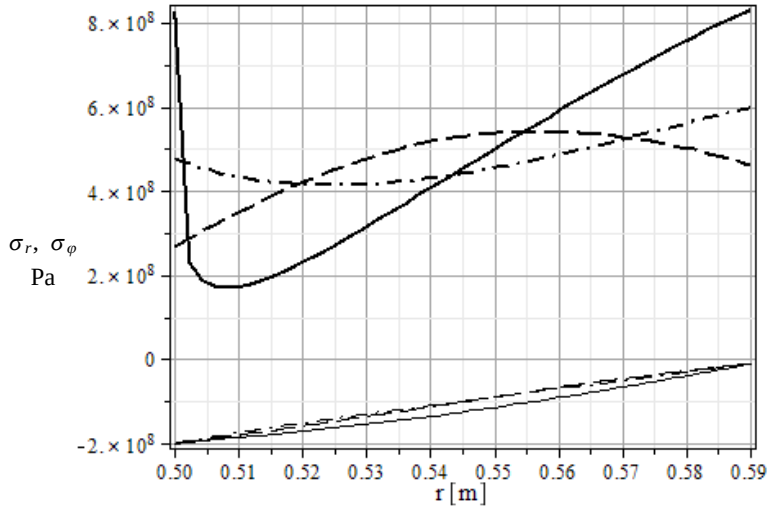

Figure 4. The radial and tangential normal stresses within the spherical pressure vessels

Example 2. In the second numerical example a functionally graded orthotropic disk is considered and the results of the analytical solution and the numerical method are compared to each other. The following numerical data were used:

$$C^0_{110} = 0.44\,\text{GPa},\ \ C^0_{120} = 0.32\,\text{GPa},\ \ C^0_{220} = 16.266\,\text{GPa},$$
$$\rho^0_0 = 4000\frac{\text{kg}}{\text{m}^3},\ \ \beta^0_{10} = -12476\frac{\text{N}}{\text{m}^2\text{K}},\ \ \beta^0_{20} = -32500\frac{\text{N}}{\text{m}^2\text{K}},$$
$$a = 0.02\text{m},\ \ b = 0.1\text{m},\ \ h(r) = 10^{-3}r^{-0.2}\,[\text{m}]\,,$$

$$p_1 = 40\text{MPa},\ p_2 = 5\text{MPa},\ \omega = 100\frac{1}{\text{s}},\ t_1 = 120\text{ K}, t_2 = 20\text{K}$$

$$\lambda(r) = \frac{20}{a^{0.2}} r^{0.2} \left[\frac{\text{W}}{\text{mK}}\right],\ \vartheta(r) = \frac{70}{a^{0.2}} r^{0.2} \left[\frac{\text{W}}{\text{m}^2\text{K}}\right],\ t_{env}(r) = 95 - 3000 r^{1.8}\ [\text{K}],\ n = 12.$$

The results can be seen in Figures 5 and 6. The numerical and analytical results are in good agreement. The average relative error is around 0.01 percent with the Runge-Kutta-Fehlberg method.

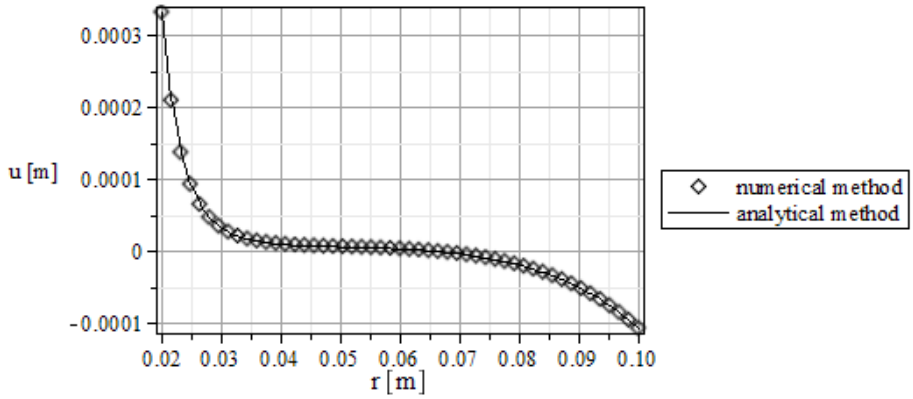

Figure 5. Results of the numerical and analytical methods for the radial displacement fields

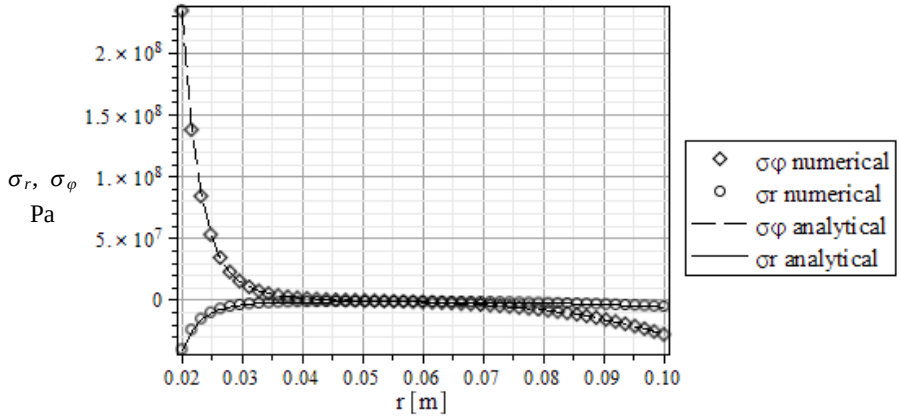

Figure 6. Results of the numerical and analytical methods for the normal stresses

Example 3. For the last example a monoclinic material is considered where the material properties are specific functions of the radial coordinate and the temperature.

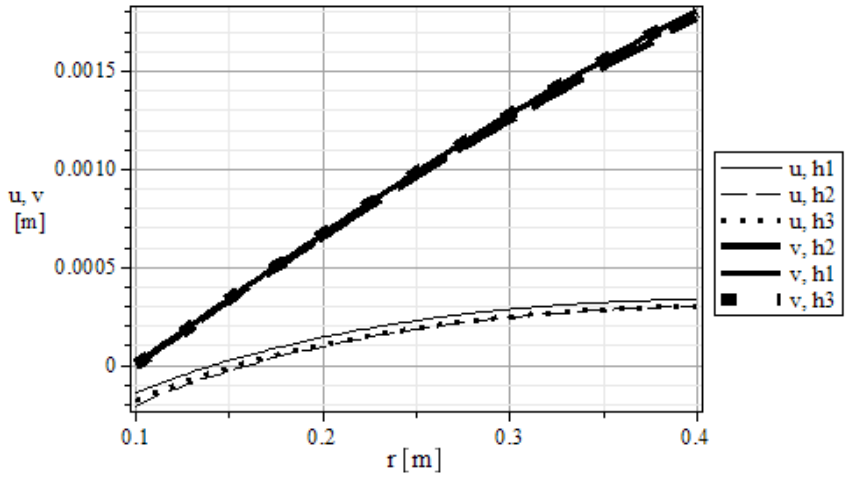

Figure 7. Curves of the radial and tangential displacements

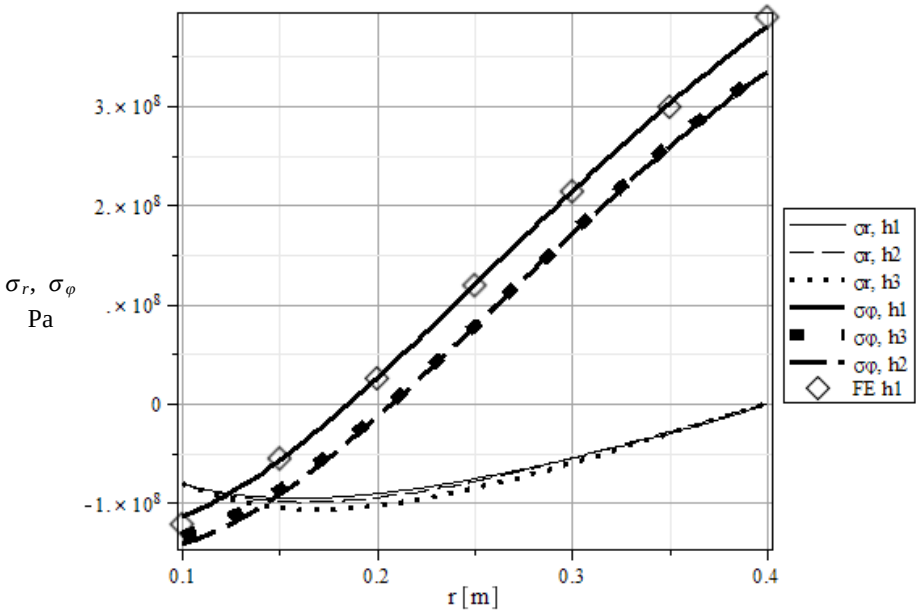

Figure 8. Curves of the radial and tangential normal stresses

The material parameters, geometry and loading are:

$$Z(r,T) = \left(1 + \frac{0.22T}{100}\right)\left(\frac{r}{R_1}\right)^m, \quad C_{11} = 26.43Z(r,T)\,\text{GPa},$$

$$C_{12} = 13,57Z(r,T), \quad \text{GPa}, \quad C_{22} = 35.7Z(r,T)\,\text{GPa}$$

$$C_{16} = 2.495Z(r,T)\,\text{GPa},\ \ C_{26} = 3.163Z(r,T)\,\text{GPa}$$

$$C_{66} = 8.49Z(r,T)\,\text{GPa},\ \ \rho = 4000Z(r,T)\frac{\text{kg}}{\text{m}^3},$$

$$\beta_1 = -8.03\cdot 10^5 Z(r,T)\frac{\text{N}}{\text{m}^2\text{K}},\ \ \beta_2 = -5.234\cdot 10^5 Z(r,T)\frac{\text{N}}{\text{m}^2\text{K}},$$

$$\beta_6 = -3.026\cdot 10^5 Z(r,T)\frac{\text{N}}{\text{m}^2\text{K}},$$

$$R_1 = 0.1\text{m},\ \ R_2 = 0.4\text{m},\ \ p_1 = 80\text{MPa},\ \ p_2 = 0\text{MPa}$$

$$\omega = 100\frac{1}{\text{s}},\ \ T(r) = -99 - 130\ln(r),\ \ m = 2,$$

$$h_1(r) = -0.266r + 0.01266,\ \ h_2(r) = 0.0115 - 0.0033e^{2r},\ \ h_3(r) = 0.033r^{-0.4}.$$

Three different profiles are investigated with the same volume. The displacement coordinates u, v and the normal stresses are illustrated in Figures 7 and 8. The calculations were checked by results obtained by Abaqus. The disk was modeled with 3D coupled temperature-displacement elements and the body was built from 32 homogeneous temperature-dependent bonded layers. The results are in good agreement, although the tangential normal stresses from the FE method oscillated at the ends of the disk due to the multilayered approach.

With the developed method, the optimal profile for a specific load set can be calculated effectively when used in conjunction with optimization codes.

6. Conclusions

A numerical method was presented to obtain the solution of steady-state thermoelastic problems for radially graded spherical pressure vessels and rotating cylindrically monoclinic disks. A new numerical approach was presented which is based on a coupled system of first-order ordinary differential equations with the displacement and the stress function as unknowns. The original axisymmetric two-point boundary value problem was transformed to an initial value problem based on the basic equations of thermoelasticity and plane-stress state in order to calculate the displacement and stress field. The material properties of spherical bodies and anisotropic disks are arbitrary functions of the radial coordinate and the temperature. The developed methods were checked by an analytical solution of an orthotropic disk where the material distribution follows a power-law function. The results were compared to each other and to results obtained by finite element simulations and they are in good agreement.

References

1. Hetnarski, R. B. and Eslami, M. R. *Thermal Stresses – Advanced Theory and Applications*. Springer, New York, 2010.
2. Lekhnitskii, S. G. *Theory of Elasticity of an Anisotropic Body*. Mir Publishers, Moscow, 1981.
3. Noda, N., Hetnarski, R. B., and Tanigawa, Y. *Thermal Stresses*. Rochester, New York, USA: Lastran Corporation, 2000.

4. Obata, Y. and Noda, N. "Steady thermal stresses in a hollow circular cylinder and a hollow sphere of a functionally gradient materiaL." *Journal of Thermal Stresses,* **17**(4), (1994), 471–487. doi: 10.1080/01495739408946273.
5. Kim, K.S. and Noda, N. "Green's function approach to unsteady thermal stresses in an infinite hollow cylinder of functionally graded material." *Acta Mechanika,* **156**, (2002), pp. 145–161. doi: 10.1007/BF01176753.
6. Chen, Y. Z. and Lin, X. Y. "Elastic analysis for thick cylinders and spherical pressure vessels made of functionally graded materials." *Computational Materials Science,* **44**, (2008), 581–587. doi: 10.1016/j.commatsci.2008.04.018.
7. Nayak, P., Mondal, S. C., and Nandi, A. "Stress, Strain and displacement of a functionally graded thick spherical vessel." *Engineering Science and Technology,* **3**(4), (2011), pp. 2660–2671.
8. Bayat, Y., Ghannad, M., and Torabi, H. "Analytical and numerical analysis for the FGM thick sphere under combined pressure and temperature loading." *Archive of Applied Mechechanics,* **10**, (2011), pp. 229–242. doi: 10.1007/s00419-011-0552-x.
9. Pen, X. and Li, X. "Thermoelastic analysis of functionally graded annulus with arbitrary gradient." *Applied Mathematics and Mechanics (English Edition),* **30**(10), (2010), pp. 1211–1220.
10. Nejad, M. Z. and Theotokoglou, E.E. "The radially nonhomogeneous thermoelastic axisymmetric problem." *International Journal of Mechanical Sciences,* **120**, (2017), pp. 311–321. doi: 10.1016/j.ijmecsci.2016.11.010.
11. Bayat, Y., Jabbari, M., and Ghannad, M. "A general disk form formulation for thermo-elastic analysis of functionally graded thick shells of revolution with arbitrary curvature and variable thickness." *Acta Mechanica,* **228**(1), (2017), pp. 215–231. doi: 10.1007/s00707-016-1709-z.
12. Jabbari, M., Nejad, M.Z., and Ghannad, M. "Thermo-elastic analysis of axially functionally graded rotating thick truncated conical shells with varying thickness." *Composites Part B: Engineering,* **96**, (2016), 20–34. doi: 10.1016/j.compositesb.2016.04.026.
13. Dai, T. and Dai, H. L. "Thermo-elastic analysis of a functionally graded rotating hollow circular disk with variable thickness and angular speed." *Applied Mathematical Modelling,* **40**, (2016), pp. 7689–7707. doi: 10.1016/j.apm.2016.03.025.
14. Boğa, C. and Yildirim, V. "Application of the complementary functions method to an accurate elasticity solution for the radially functionally graded (FG) rotating disks with continuously variable thickness and density." *Solid State Phenomena,* **250**, (2016), pp. 100–105. doi: 10.4028/www.scientific.net/SSP.251.100.
15. Gönczi, D. and Ecsedi, I. "Thermoelastic analysis of functionally graded hollow circular disk." *Archive of Mechanical Engineering,* **62**(1), (2015), pp. 5–18. doi: 10.1515/meceng-2015-0001.
16. Çallioğlu, H., Bektaş, N. B., and Sayer, M. "Stress analysis of functionally graded rotating discs: analytical and numerical solutions." *Archive of Mechanical Engineering,* **27**, (2011), pp. 950–960. doi: 10.1007/s10409-011-0499-8.

17. Jabbari, M., Ghannad, M., and Nejad, M. "Effect of thickness profile and FG function on rotating disks under thermal and mechanical loading." *Journal of Mechanics,* **32**(1), (2016), pp. 35–46. DOI: 10.1017/jmech.2015.95.
18. Vandana, G. and Singh, S.B. "Mathematical modeling of creep in a functionally graded rotating disc with varying thickness." *Regenerative Engineering and Translational Medicine,* **2**(3), (2016), pp. 126–140. DOI: 10.1007/s40883-016-0018-3.
19. Manish, Garg. "Stress analysis of variable thickness rotating FG disc." *International Journal of Pure and Applied Physics,* **13**(1), (2017), pp. 158–161.
20. Zheng, Y., Bahaloo, H., Mousanezhad, D., Mahdi, E., Vaziri, A., and Nayeb-Mashemi, H. "Stress analysis in functionally graded rotating disks with non-uniform thickness and variable angular velocity." *International Journal of Mechanical Sciences,* **119**, (2017), pp. 283–293. DOI: 10.1016/j.ijmecsci.2016.10.018.
21. Zheng, Y., Bahaloo, H., Mousanezhad, D., Mahdi, E., Vaziri, A., and Nayeb-Mashemi, H. "Displacement and stress fields in a functionally graded fiber-reinforced rotating disk with nonuniform thickness and variable angular velocity." *International Journal of Mechanical Sciences,* **139**(3), (2017). DOI: 10.1115/1.4036242.
22. Eraslan, A. N., Kaya, Y., and Varli, E. "Analytical solutions to orthotropic variable thickness disk problems." *Pamukkale University Journal of Engineering Sciences,* **22**(1), (2016), pp. 24–30. DOI: 10.5505/pajes.2015.91979.
23. Tarn, J. Q. "Exact solutions for functionally graded anisotropic cylinders subjected to thermal and mechanical loads." *International Journal of Solids and Structures,* **38**(46-47), (2016), pp. 8189–8206. DOI: 10.1016/S0020-7683(01)00182-2.
24. Sladek, J., Sladek, V., and Zhang, Ch. "Stress analysis in anisotropic functionally graded materials by the MLPG method." *Engineering Analysis with Boundary Elements,* **29**(6), (2005), pp. 597–609. DOI: 10.1016/j.enganabound.2005.01.011.
25. Vel, S. S. "Exact thermoelastic analysis of functionally graded anisotropic hollow cylinders with arbitrary material gradation." *Mechanics of Advanced Materials and Structures,* **18**, (2011), pp. 14–31. DOI: 10.1080/15376494.2010.519218.
26. Chen, J., Ding, H., and Chen, W. "Three-dimensional analytical solution for a rotating disc of functionally graded materials with transverse isotropy." *Archive of Applied Mechanics,* **77**(4), (2007), pp. 241–251. DOI: 10.1007/s00419-006-0098-5.
27. Chang, H. H. and Tarn, J. Q. "A state space formalism and perturbation method for generalized thermoelasticity of anisotropic bodies." *International Journal of Solids and Structures,* **44**, (2007), 956–975. DOI: 10.1016/j.ijsolstr.2006.05.034.
28. Ceniga, L. "Thermal stresses in two- and three-component anisotropic materials." *Acta Mechanica Sinica,* **26**, (2010), pp. 695–709. DOI: 10.1007/s10409-010-0368-x.

29. Ceniga, L. "Thermoelastic in-plane fields in a linear anisotropic solid." *International Journal of Engineering Science,* **69**, (2013), pp. 43–60. doi: 10.1016/j.ijengsci.2013.03.012.
30. Yildirim, V. "The complementary functions method (CFM) solution to the elastic analysis of polar orthotropic rotating discs." *Journal of Applied and Computational Mechanics,* **4**(3), (2018), pp. 216–230. doi: 10.22055/JACM.2017.23188.1150.
31. Allam, M. N. M., Tantawy, R., and Zenkour, A. M. "Thermoelastic stresses in functionally graded rotating annular disks with variable thickness." *Journal of Theoretical and Applied Mechanics,* **56**(4), (2019), pp. 1029–1041. doi: 10.15632/jtam-pl.56.4.1029.
32. Sondhi, L., Thawait, A. K., Sanyal, S., and Bhowmick, S. "Stress and deformation analysis of variable thickness clamped rotating disk of functionally graded orthotropic material." *Materials Today: Proceedings,* **18**(7), (2019), pp. 4431–4440. doi: 10.1016/j.matpr.2019.07.412.
33. Nayak, P., Bhowmick, P., Saha, K. N., and Bhowmick, S. "Elasto-plastic analysis of thermo-mechanically loaded functionally graded disks by an iterative variational method." *Engineering Science and Technology, an International Journal,* **23**(1), (2019), pp. 42–64. doi: 10.1016/j.jestch.2019.04.007.
34. Kiss, L. P. "Nonlinear stability analysis of FGM shallow arches under an arbitrary concentrated radial force." *International Journal of Mechanics and Materials in Design,* **16**(1), (2020), pp. 901–108. doi: 10.1007/s10999-019-09460-2.
35. Alimoradzadeh M., Saledi, M., and Esfarjani, S. M. "Nonlinear vibration analysis of axially functionally graded microbeams based on nonlinear elastic foundation using modified couple stress theory." *Periodica Polytechnica Mechanical Engineering,* **64**(2), (2020), pp. 97–108. doi: 10.3311/PPme.11684.
36. Carslaw, H. S. and Jaeger, I. C. *Conduction of Heat in Solids.* Clarendon Press, Oxford, 1959.
37. Shen, H. S. *Functionally Graded Materials: Nonlinear Analysis of Plates and Shells.* CRC Press, London, UK, 2009. doi: 10.1201/9781420092578.
38. Touloukian, Y. S., Gerritsen, J. K., and Moore, N. Y. *Thermophysical Properties Research Literature Retrieval Guide.* New York, Plenum Press, 1967.
39. Gönczi, D. "Thermoelastic Problems of Functionally Graded and Composite Structural Components." PhD dissertation. University of Miskolc, 2017.